

University of Groningen

## The decay of the 21.47-MeV stretched resonance in $^{13}\text{C}$

Cieplicka-Oryńczak, N.; Jaganathen, Y.; Fornal, B.; Leoni, S.; Płoszajczak, M.; Ciemała, M.; Ziliani, S.; Kmiecik, M.; Maj, A.; Łukasik, J.

*Published in:*

Physics Letters, Section B: Nuclear, Elementary Particle and High-Energy Physics

*DOI:*

[10.1016/j.physletb.2022.137398](https://doi.org/10.1016/j.physletb.2022.137398)

**IMPORTANT NOTE: You are advised to consult the publisher's version (publisher's PDF) if you wish to cite from it. Please check the document version below.**

*Document Version*

Publisher's PDF, also known as Version of record

*Publication date:*

2022

[Link to publication in University of Groningen/UMCG research database](#)

*Citation for published version (APA):*

Cieplicka-Oryńczak, N., Jaganathen, Y., Fornal, B., Leoni, S., Płoszajczak, M., Ciemała, M., Ziliani, S., Kmiecik, M., Maj, A., Łukasik, J., Pawłowski, P., Sowicki, B., Wasilewska, B., Ziębliński, M., Bednarczyk, P., Boiano, C., Bottoni, S., Bracco, A., Brambilla, S., ... Włoch, B. (2022). The decay of the 21.47-MeV stretched resonance in  $^{13}\text{C}$ : A precise probe of the open nuclear quantum system description. *Physics Letters, Section B: Nuclear, Elementary Particle and High-Energy Physics*, 834, [137398]. <https://doi.org/10.1016/j.physletb.2022.137398>

### Copyright

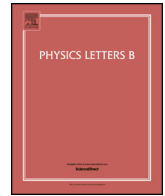
Other than for strictly personal use, it is not permitted to download or to forward/distribute the text or part of it without the consent of the author(s) and/or copyright holder(s), unless the work is under an open content license (like Creative Commons).

The publication may also be distributed here under the terms of Article 25fa of the Dutch Copyright Act, indicated by the "Taverne" license. More information can be found on the University of Groningen website: <https://www.rug.nl/library/open-access/self-archiving-pure/taverne-amendment>.

### Take-down policy

If you believe that this document breaches copyright please contact us providing details, and we will remove access to the work immediately and investigate your claim.

Downloaded from the University of Groningen/UMCG research database (Pure): <http://www.rug.nl/research/portal>. For technical reasons the number of authors shown on this cover page is limited to 10 maximum.



## The decay of the 21.47-MeV stretched resonance in $^{13}\text{C}$ : A precise probe of the open nuclear quantum system description

N. Cieplicka-Oryńczak<sup>a,\*</sup>, Y. Jaganathen<sup>a,i</sup>, B. Fornal<sup>a</sup>, S. Leoni<sup>b</sup>, M. Płoszajczak<sup>c</sup>,  
M. Ciemała<sup>a</sup>, S. Ziliani<sup>b</sup>, M. Kmiecik<sup>a</sup>, A. Maj<sup>a</sup>, J. Łukasik<sup>a</sup>, P. Pawłowski<sup>a</sup>, B. Sowicki<sup>a</sup>,  
B. Wasilewska<sup>a</sup>, M. Ziębliński<sup>a</sup>, P. Bednarczyk<sup>a</sup>, C. Boiano<sup>b</sup>, S. Bottoni<sup>b</sup>, A. Bracco<sup>b</sup>,  
S. Brambilla<sup>b</sup>, I. Burducea<sup>e</sup>, F. Camera<sup>b</sup>, I. Ciepał<sup>a</sup>, C. Clisu<sup>e</sup>, F.C.L. Crespi<sup>b</sup>,  
K. Dhanmeher<sup>a</sup>, N. Florea<sup>e</sup>, E. Gamba<sup>b</sup>, J. Grębosz<sup>a</sup>, M.N. Harakeh<sup>d</sup>, D.A. Iancu<sup>e</sup>,  
Ł.W. Iskra<sup>a</sup>, M. Krzysiek<sup>a</sup>, P. Kulesa<sup>f</sup>, N. Marginean<sup>e</sup>, R. Marginean<sup>e</sup>, I. Matea<sup>g</sup>,  
M. Matejska-Minda<sup>a</sup>, K. Mazurek<sup>a</sup>, B. Million<sup>b</sup>, W. Parol<sup>a</sup>, M. Sferrazza<sup>h</sup>, L. Stan<sup>e</sup>,  
B. Włoch<sup>a</sup>

<sup>a</sup> Institute of Nuclear Physics Polish Academy of Sciences, Radzikowskiego 152, PL-31342 Krakow, Poland

<sup>b</sup> Università degli Studi di Milano and INFN Sezione di Milano, Via Celoria 16, 20133 Milano, Italy

<sup>c</sup> Grand Accélérateur National d'Ions Lourds, CEA/DSM-CNRS/IN2P3, BP 55027, F-14076 Caen Cedex, France

<sup>d</sup> Nuclear Energy Group, ESRIG, University of Groningen, Zernikelaan 25, NL-9747 AA Groningen, the Netherlands

<sup>e</sup> "Horia Hulubei" National Institute for Physics and Nuclear Engineering, RO-077125 Bucharest-Magurele, Romania

<sup>f</sup> Institut für Kernphysik, 52425 Jülich, Germany

<sup>g</sup> Université Paris-Saclay, CNRS/IN2P3, IJCLab, 91405 Orsay, France

<sup>h</sup> Université Libre de Bruxelles, B-1050 Brussels, Belgium

<sup>i</sup> National Centre for Nuclear Research, Pasteura 7, 02-093 Warsaw, Poland

### ARTICLE INFO

#### Article history:

Received 9 May 2022

Received in revised form 21 August 2022

Accepted 21 August 2022

Available online 24 August 2022

Editor: D.F. Geesaman

#### Keywords:

$^{13}\text{C}$

Nuclear structure

Stretched resonance states

Gamow Shell Model

### ABSTRACT

The decay of the 21.47-MeV stretched resonance in  $^{13}\text{C}$ , arising from  $p_{3/2} \rightarrow d_{5/2}$  nucleon excitation coupled to maximum spin, was investigated in a  $(p, p')$  experiment at 135 MeV proton bombarding energy, performed at the Cyclotron Centre Bronowice (CCB) at IFJ PAN in Krakow. First experimental information on the proton and neutron decay branches from this state was obtained by using coincidence measurement of protons inelastically scattered on a  $^{13}\text{C}$  target and  $\gamma$  rays from daughter nuclei, namely,  $^{12}\text{B}$  (proton decay) and  $^{12}\text{C}$  (neutron decay). The main branches lead to the  $J^\pi = 2^+$ , first-excited state at 0.953 MeV in  $^{12}\text{B}$ , and to the  $J^\pi = 1^+$ ,  $T = 1$  level at 15.110 MeV in  $^{12}\text{C}$ . The results were compared with predictions from the Gamow Shell Model (GSM), which was used to describe the stretched resonance in terms of its energy, width, electromagnetic transition strengths and decay pattern. A very good agreement was obtained between the measured and calculated properties of the 21.47-MeV stretched resonance in  $^{13}\text{C}$ , demonstrating the high-quality and precision of the GSM wave function calculations, which include coupling to the resonant and non-resonant particle continuum.

© 2022 The Authors. Published by Elsevier B.V. This is an open access article under the CC BY license (<http://creativecommons.org/licenses/by/4.0/>). Funded by SCOAP<sup>3</sup>.

Nuclei are quantum many-body systems with both bound and unbound states, namely excitations located below and above the lowest particle emission threshold, respectively. The latter are resonant states lying in the continuum, the understanding of which goes beyond the traditional configuration interaction approaches in the closed quantum system approximation, such as the standard

nuclear Shell Model (SM) [1–3]. In this excitation energy regime, the coupling to the decay channels and scattering continuum has a direct impact on the structure of nuclear states and requires an open quantum system (OQS) description.

In light nuclei, while the low-lying bound structures can be predicted by state-of-the-art *ab initio* as well as large-scale shell-model calculations [4–8] a comprehensive description of bound, unbound states and reaction observables, which are crucial for understanding stellar nucleosynthesis, is offered, for example, by the GSM [9–15].

\* Corresponding author.

E-mail address: natalia.cieplicka@ifj.edu.pl (N. Cieplicka-Oryńczak).

Particular unbound excitations, named “stretched states”, of interest here, are an excellent testing ground for the GSM, the predictive power of which has not been fully tested. These states are single-particle excitations dominated by a single particle-hole component, for which both the excited particle and the residual hole occupy the highest angular-momentum orbitals  $j_p$  and  $j_h$  in their respective shells, and couple to  $J_{max} = j_p + j_h$ . Examples of high-multipolarity transitions to stretched states are  $M4$  transitions in  $1p$ -shell nuclei ( $1p_{3/2} \rightarrow 1d_{5/2}$ ), and  $M6$  transitions in  $2s1d$ -shell nuclei ( $1d_{5/2} \rightarrow 1f_{7/2}$ ) [16,17]. Due to the expected low density of other one-particle-one-hole configurations of high angular momenta in the energy region where stretched states appear, their configurations should be relatively simple. This feature makes stretched states very attractive, as their theoretical analysis could provide clean information about the role of continuum couplings in stretched excitations, including details on isospin properties, radial overlap integrals, spectroscopic factors, transitions amplitudes and densities [18].

The excitation of stretched states is enhanced in inelastic scattering reactions at large momentum transfer. A few stretched configurations have been identified in  $p$ -shell nuclei (such as C, N, O) by using this method [16,18,19]. The decay of stretched resonances in light systems is expected to be dominated by the direct decay of proton and neutron over the statistical (compound nucleus) decay; however, the experimental information on this matter is still largely missing.

In this work, we study the  $^{13}\text{C}$  nucleus, which is one of the very few odd- $A$  nuclei for which compelling evidence for inelastic excitations to stretched states was gathered. Here, the states at 9.50, 16.08, and 21.47 MeV were identified as arising from  $p_{3/2} \rightarrow d_{5/2}$  nucleon excitations into stretched configurations, following inelastic pion [20,21], proton [22], and electron scattering [23]. The 9.5-MeV and 16.08-MeV states (with width of  $< 5$  keV and 150(15) keV, respectively) were suggested to be a  $J^\pi = 9/2^+$ ,  $T = 1/2$  pure neutron excitation and a  $J^\pi = (7/2^+)$ ,  $T = (1/2)$  excitation of mainly proton character, respectively [23,20], while the study of  $(\pi, \pi')$  scattering cross sections showed that the 21.47-MeV state contains both proton and neutron components [20]. For this 21.47-MeV excitation (with a width of 270(20) keV), spin and isospin are uncertain, as  $J^\pi = (7/2^+, 9/2^+)$  and  $T = (1/2, 3/2)$  values are both possible. The isospin composition of this state was investigated by measuring its neutron decay in the  $^{12}\text{C}(p, \pi^+)$  reaction, with no conclusive results [24]. In our work, we concentrate on the 21.47-MeV  $M4$  resonance, which is the most strongly populated in  $(p, p')$  reaction and is well separated from other nearby excitations [22]. Decay branchings to states in  $^{12}\text{B}$  and  $^{12}\text{C}$  daughter nuclei have been extracted by measuring the succeeding decay  $\gamma$  rays following the proton and neutron emission, respectively. They have been compared with predictions of GSM calculations, here performed for the first time for a stretched state, resulting in a good description of the resonance energy, width and decay pattern.

The 21.47-MeV stretched resonance in  $^{13}\text{C}$  was populated in the proton inelastic scattering  $^{13}\text{C}(p, p')$  reaction at the Cyclotron Centre Bronowice (CCB) at IFJ PAN in Krakow. The 135-MeV proton beam from the cyclotron Proteus C-235 was focused on a  $^{13}\text{C}$  target with thickness of 197 mg/cm<sup>2</sup>, while the KRATTA telescope array [25], composed of six modules of charged-particle CsI triple telescopes, was placed at around 36° with respect to the beam axis. At this angle the angular distribution of the scattered protons, associated with the population of the 21.47-MeV state in  $^{13}\text{C}$ , should reach its maximum [22]. The  $\gamma$  rays from the reaction products were measured by four LaBr<sub>3</sub> detectors [26] and two clusters of the PARIS scintillator array [27]. Part of the data were also taken with a thin 1 mg/cm<sup>2</sup>  $^{13}\text{C}$  target, in order to detect light

charged particles from the resonance decay using a 1.5 mm thick position-sensitive double-sided silicon strip detector (DSSSD).

The excitation energy spectrum of  $^{13}\text{C}$  was constructed from the measured energy of the scattered protons, as shown in Fig. 1(b). The 21.47-MeV stretched resonance appears here as a well-isolated peak in the spectrum. Next, proton (in KRATTA) and  $\gamma$ -coincidence data were sorted into a two-dimensional matrix  $(E^*, E_\gamma)$ , with the  $^{13}\text{C}$  excitation energy ( $E^*$ ) on the horizontal and the  $\gamma$ -ray energy ( $E_\gamma$ ) on the vertical axis, respectively (see Fig. 1(a)). Projections on the excitation-energy and gamma-energy axes are presented on the top and on the right of Fig. 1(a).

As illustrated in Fig. 2, the decay of the  $M4$  stretched state at 21.47 MeV in  $^{13}\text{C}$  may proceed via  $p$ ,  $n$ ,  $d$ , and  $\alpha$  particle emission to excited or ground states in  $^{12}\text{B}$ ,  $^{12}\text{C}$ ,  $^{11}\text{B}$ , and  $^9\text{Be}$ , respectively. To access the branchings to the excited states, we studied the  $\gamma$  rays emitted from these products, in coincidence with inelastically-scattered protons populating the 21.47-MeV resonance.

Because of the high proton separation energy in  $^{13}\text{C}$  ( $S_p = 17.533$  MeV), one may expect population of only low-lying bound states in  $^{12}\text{B}$ , namely the 0.953, 1.674, 2.621, and 2.723 MeV excitations having spin-parity values  $2^+$ ,  $2^-$ ,  $1^-$ , and  $0^+$ , respectively. The  $\gamma$  decay from the 0.953-MeV state to the ground state (g.s.) is clearly seen in the projection spectrum of Fig. 1(a), while the  $\gamma$  rays from the decay of the 1.674- and 2.621-MeV states, with energies of 1.674 and 1.668 MeV, are seen as a peak at  $\sim 1.7$  MeV. They could not be separated due to the energy resolution (FWHM) of the scintillator detectors of approximately 40 keV. A gate set on the 0.953-MeV  $\gamma$  ray in the  $^{13}\text{C}(E^*, E_\gamma)$  matrix (Fig. 1(a)) displays a strong coincidence with the 21.47-MeV resonance, over a background corresponding to the decay from other unbound states above the proton-decay threshold (see Fig. 1(f)).

For the neutron-decay channel leading to  $^{12}\text{C}$ ,  $\gamma$  transitions are expected from the  $2^+$  at 4.440 MeV and  $1^+$  at 15.110 MeV states, which decay to the ground state via the 4.439- and 15.100-MeV  $\gamma$  rays, respectively. The spectrum gated on the 4.439-MeV  $\gamma$  ray (Fig. 1(d)) shows no evidence of the 21.47-MeV resonance. The peak corresponding to the resonance is instead visible (over a background from other unbound states) when a gate is set on the 15.100-MeV  $\gamma$  ray (Fig. 1(c)). We note that other neutron decay branches from the 21.47-MeV resonance populate states in  $^{12}\text{C}$  which decay primarily by low-energy protons, leading to the first-excited state at 2.125 MeV and the ground state of  $^{11}\text{B}$ , or by  $\alpha$  particles populating the  $^8\text{Be}$  nucleus. In the case of  $^{11}\text{B}$ , a gate set on the 2.124-MeV  $\gamma$  transition does not reveal any coincidence with the 21.47-MeV resonance (see Fig. 1(e)), probably as a consequence of the very small energy window for a sequential neutron-proton decay (0.567 MeV for protons and 0.102 MeV for neutrons). This observation also tells us that no deuteron emission to the 2.125-MeV state in  $^{11}\text{B}$  (with 0.666 MeV deuteron energy) takes place. In the case of  $^8\text{Be}$ , there are no states emitting  $\gamma$  rays which can be populated by the 21.47-MeV resonance decay. Therefore, this route of decay cannot be traced by  $\gamma$  rays. For a similar reason, the  $\alpha$ -decay channel of the 21.47-MeV resonance leading to  $^9\text{Be}$  cannot be detected by measuring  $\gamma$  rays.

A quantitative analysis of the decay branches from the 21.47-MeV resonance, discussed above, resulted in the following relative yields (assuming 100 for the total yield of the decays observed via  $\gamma$  emission): 69(6) for the population of the 0.953-MeV  $^{12}\text{B}$  state, 7(2) distributed between the 2.621-MeV or 1.674-MeV  $^{12}\text{B}$  states, and 24(5) for the population of the  $1^+$  state at 15.110 MeV in  $^{12}\text{C}$ .

To estimate the decay branches from the 21.47-MeV resonance to ground states or excited states of daughter nuclei, not followed by  $\gamma$  decay, data on light charged particles collected with the thin  $^{13}\text{C}$  target and the DSSSD detector were used. Particle-identification matrices were constructed employing the risetime

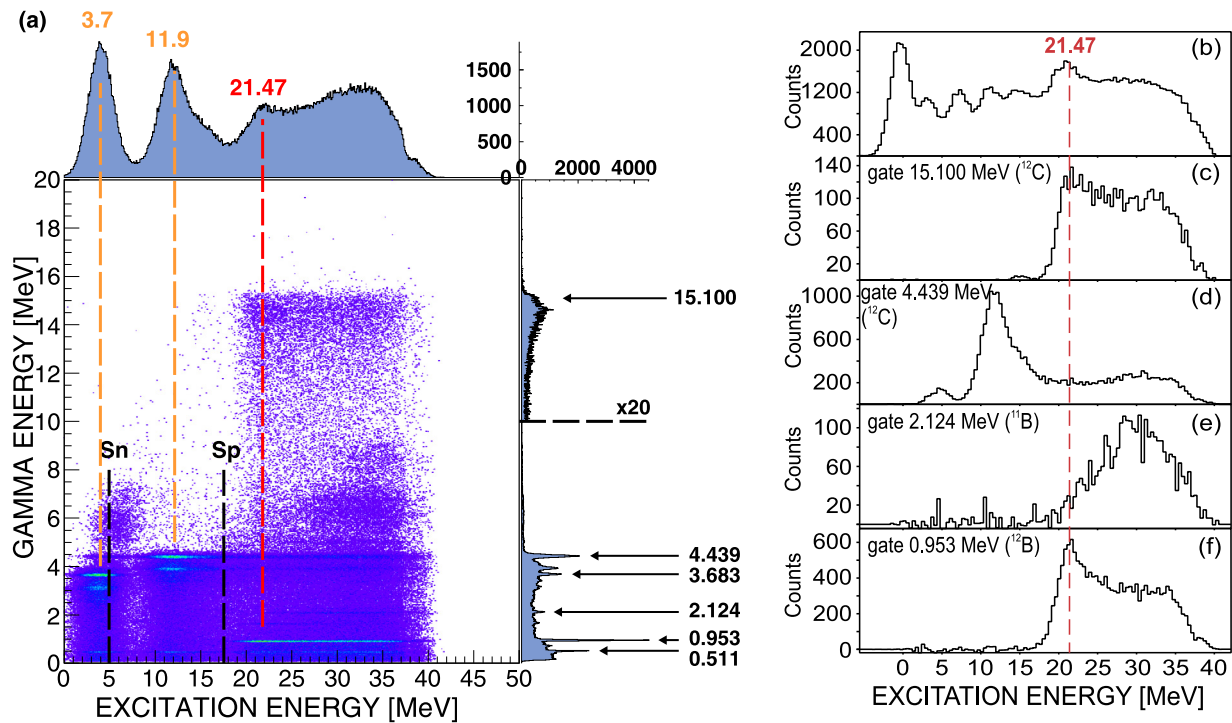


**Fig. 1.** (a) Two-dimensional matrix showing the energy of the  $\gamma$  rays detected in the scintillator detectors vs.  $^{13}\text{C}$  excitation energy reconstructed from the energy of scattered protons. Projections on the x axis (excitation energy) and y axis ( $\gamma$  energy) are shown on the top and on the right, respectively. Particle emission thresholds for neutron and proton are given, as well as the location of the 21.47-MeV stretched resonance and of the groups of excited states at 3.7 and 11.9 MeV in  $^{13}\text{C}$ , which are followed by  $\gamma$  decays. Labels on the  $\gamma$  spectrum (on the right) point to  $\gamma$  rays from excited states in  $^{12,13}\text{C}$  and  $^{12}\text{B}$ . (b)  $^{13}\text{C}$  excitation energy spectrum constructed from the energy of scattered protons measured as singles (no coincidence with  $\gamma$  rays required). (c)-(f)  $^{13}\text{C}$  excitation energy spectra obtained by gating on the  $\gamma$  transitions from  $^{12}\text{C}$  and  $^{11,12}\text{B}$  daughter nuclei, as given in the legends.

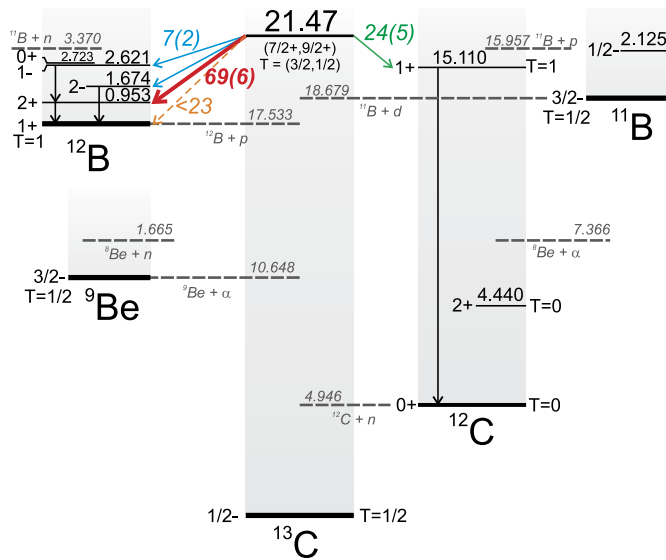


**Fig. 2.** The experimental decay scheme of the 21.47-MeV stretched resonance in  $^{13}\text{C}$  associated with the detection of  $\gamma$  rays from daughter nuclei. Relative intensities of the decay branches are obtained summing to 100 the relative yields of the decays observed via  $\gamma$  emission (see text for details).

difference technique [28]. Fig. 3(a) displays data collected by one strip in the thick-target run in single mode, while the inset shows the same matrix for events in coincidence with scattered protons detected in the KRATTA array. Only a very small fraction of events comes from  $\alpha$  particles, due to absorption in the thick target.

Fig. 3(b) shows the energy spectrum of protons in DSSSD in coincidence with scattered protons in KRATTA, populating the

21.47-MeV resonance. A peak, observed at 3 MeV, very likely corresponds to the direct population of the first-excited state in  $^{12}\text{B}$  from the 21.47-MeV resonance. This is consistent with the  $\gamma$ -ray analysis which gave a large relative yield of 69(6)% for this branch (see Fig. 2). A direct branch to the  $^{12}\text{B}$  ground state would produce a peak at 4 MeV, which is not observed here. Considering the acquired statistics in the DSSSD proton spectrum, which is very limited, the upper limit for the decay branch leading to the ground state of  $^{12}\text{B}$  is estimated to be 1/3 of the first-excited state population.

Concerning the  $\alpha$  decay from the 21.47-MeV resonance in  $^{13}\text{C}$ , one may expect direct branches to the excited particle unbound states and the ground state of the  $^9\text{Be}$  daughter nucleus. In such cases, the corresponding  $\alpha$ -particle energies would be at most 10.8 MeV (direct ground-state population). However, no traces of peaks which might be associated with  $\alpha$  decay to specific states were observed in the light-charged-particle energy spectrum. The 21.47-MeV resonance could also decay to the ground state of  $^{11}\text{B}$  via emission of the 2.79-MeV deuteron, which is not visible.

An attempt to establish the part of the resonance decay which is not associated with  $\gamma$ -ray emission in daughter nuclei was undertaken by using the single proton spectrum of Fig. 1(b), the efficiency of the  $\gamma$ -detection system and the acquisition-system dead time. It resulted in an estimated decay fraction of 46(10)%, involving  $\gamma$ -ray emission from daughter nuclei out of the total resonance population.

Fig. 2 summarizes the decay scheme of the 21.47-MeV stretched resonance in  $^{13}\text{C}$  resulting from the analysis of our experimental data. As discussed above, most of the observed intensity of the resonance decay is associated with the population via proton emission of the  $J^\pi = 2^+$ , first-excited state in  $^{12}\text{B}$ , while the neutron decay feeds the  $1^+$ ,  $T = 1$  level at 15.110 MeV in  $^{12}\text{C}$ , only. This observation and the absence of the neutron-decay branch leading



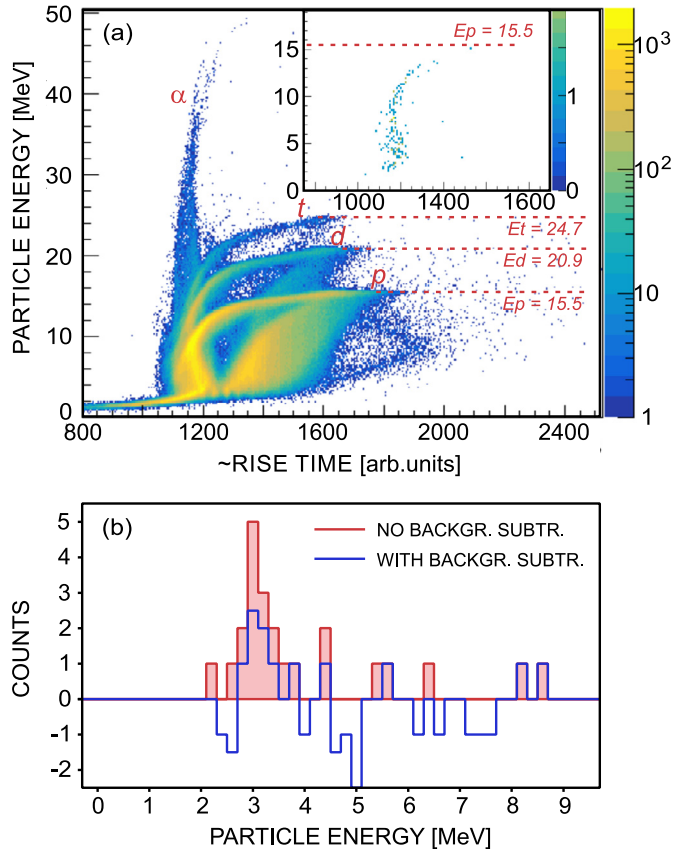


**Fig. 3.** (a) Particle identification matrix obtained from the thick target  $^{13}\text{C}(p, p')$  experiment at 135 MeV (representative example for one strip). The punch-through energies for protons ( $E_p$ ), deuterons ( $E_d$ ) and tritons ( $E_t$ ) are given by dashed lines. The inset shows the same matrix, but displayed only for the events in coincidence with the scattered proton detected in the KRATTA array. (b) In red, light-particle energy spectrum from the decay of the 21.47-MeV stretched resonance in  $^{13}\text{C}$ , without background subtraction (thin-target experiment). In blue, same spectrum, background subtracted. The peak at  $\sim 3$  MeV, corresponds to protons which populate the  $2_1^+$  state at 0.953 MeV in  $^{12}\text{B}$ .

to the  $2^+$ ,  $T = 0$  state, at 4.440 MeV, suggest that the decay of the 21.47-MeV stretched resonance in  $^{13}\text{C}$  is governed by the isospin conservation rule, thus pointing to a  $T = 3/2$  isospin assignment for this highly-excited resonance state.

The structure of unbound stretched states, such as the resonance at 21.47 MeV in  $^{13}\text{C}$ , requires an open quantum system description. The GSM [9–15] provides such a description with a fully consistent calculation of the resonance energy and width and their mutual relation [15,29]. Until now, the GSM has mostly been used to describe low-lying states for which the decay modes are rather simple, employing schematic or realistic two-body interactions. This includes weakly-bound and unbound states in helium nuclei, halo structures and tetraneutron configurations [30–33].

The high-lying 21.47-MeV stretched state in  $^{13}\text{C}$ , of interest here, may look as being out-of-range for a GSM description, from an energy point of view. However, its relatively narrow width (270(20) keV) and simple dominant configuration make the GSM approach possible, thus providing an excellent test for the GSM description of the coupling to the different decay channels.

In the present GSM calculations, the interaction is made of two parts: a Woods-Saxon potential with a spin-orbit and a Coulomb term to model the effective  $^4\text{He}$  core, and an effective finite-range two-body potential based on the references [34,35]. This potential has central, spin-orbit and tensor Gaussian terms with different ranges to account for the low and high momentum components of the nuclear interaction and has been proven to work on large-scale

calculations in  $p$ -shell nuclei [36]. The description of  $^{13}\text{C}$  with 9 valence nucleons is very demanding computationally-wise due to the continuum discretization. Multiple truncations were also needed, to target the relatively simple stretched state.

The model space was chosen to be the  $psd + f_{7/2}$  space, built on the single particle poles  $0p_{3/2}$ ,  $0p_{1/2}$ ,  $1s_{1/2}$ ,  $0d_{5/2}$ ,  $0d_{3/2}$  and their associated continua discretized with  $\sim 25$  Gauss-Legendre points each. The  $f_{7/2}$  continuum represented by 4 harmonic oscillator shells was added to the model space to gauge any effect of the  $f$  shells on the stretched state, e.g., a possible decay to the  $1^-$  state of  $^{12}\text{B}$ , otherwise strictly forbidden. A maximum of three effective holes in the closed  $^{12}\text{C}$  shells was allowed, and additional truncations on the number of particles in the different continua based on energy considerations were performed. The 14 depths (central + spin-orbit, neutron and proton) of the one-body Woods-Saxon potential and the 7 parameters of the two-body interaction were adjusted to 49 states belonging to the low-lying spectra of  $^{12}\text{B}$ ,  $^{12,13,14}\text{C}$ ,  $^{12,13,14}\text{N}$ , and  $^{14}\text{O}$ . Following what was done in Ref. [36], the optimization procedure was based on the Gauss-Newton method coupled to the Singular Value Decomposition. The Uncertainty Quantification model based on linear regression was used to assess the statistical uncertainties here presented. The optimization yielded an r.m.s. deviation of  $\sim 397$  keV ( $\sim 207$  keV for the  $A = 12, 13$  nuclei).

Since the experimental spin-parity and isospin assignments for the 21.47 MeV stretched resonance are  $J^\pi = (7/2^+, 9/2^+)$  and  $T = (1/2, 3/2)$ , we concentrated only on the calculated  $7/2^+$  and  $9/2^+$  states. In the expected energy region between 16.5 and 26.5 MeV, four candidates were found: three resonances  $7/2^+$  (indices 6, 7 and 8) and one resonance  $9/2_3^+$ . For each of these resonances, various properties were calculated to identify the experimental M4 state. For example, the  $7/2_8^+$  at 22.1(8) MeV could be discarded because of the small percentage ( $\sim 15\%$ ) of a particle-hole excitation between the  $p_{3/2}$  and the  $d_{5/2}$  orbitals. On the contrary, the structure of the other three resonances, namely,  $7/2_6^+$  at 19.9(5) MeV,  $7/2_7^+$  at 20.9(5) MeV and  $9/2_3^+$  at 21.8(7) MeV, involves significant contribution (from 50% to 65%) of transitions from  $p_{3/2}$  to  $d_{5/2}$ , as expected for the stretched resonance. The three states have an isospin of respectively 1.44, 1.36 and 1.49, i.e., close to  $3/2$ . For each of these states, we have also calculated the spectroscopic factors ( $S_f$ ) [37]. Although the spectroscopic factors are not observables in the strictest sense [38–40], they are a reasonable indicator of the configuration mixing in the many-body wave function, and for that matter they allow for the more instructive comparison also in terms of decay pattern. The first general observation is that, for all three states considered here,  $7/2_6^+$ ,  $7/2_7^+$  and  $9/2_3^+$ , the isospin mixing is relatively small and the calculated spectroscopic factors to the  $T = 0$  states are too small to give rise to any significant branching to  $T = 0$  states, including the  $2_1^+$ ,  $T = 0$  state in  $^{12}\text{C}$ . In consequence, we concentrate on the decay to  $T = 1$  states, only.

The spectroscopic factors reveal the differences between  $7/2_6^+$  ( $\Gamma = 1500(200)$  keV) and  $7/2_7^+$  ( $\Gamma = 400(300)$  keV) resonances. The  $7/2_6^+$  state is mostly built on the  $1^+$  states of  $^{12}\text{B}$  ( $1^+ \otimes d_{5/2}$ ,  $S_f = 0.25$ ) and  $^{12}\text{C}$  ( $1^+ \otimes d_{5/2}$ ,  $S_f = 0.58$ ), while the  $7/2_7^+$  is built on the  $2_1^+$  state in  $^{12}\text{B}$  and the  $2_2^+$  state in  $^{12}\text{C}$  (see Table 1 for details). Considering that the experimental decay of the resonance at  $E_{\text{exp}} = 21.47$  MeV goes mostly to the  $2^+$  excitation in  $^{12}\text{B}$ , the  $7/2_6^+$  state is excluded.

The GSM also allows us to calculate partial widths [41], which are given in Table 1 for the  $7/2_7^+$  resonance, with the corresponding branching ratios. The uncertainties appended to those values are numerical uncertainties due to the lack of precision of the calculated GSM wave functions at large distances from which the asymptotic normalization constants and then the partial widths are extracted. On the other hand, the uncertainty ( $\Delta\Gamma = 300$  keV) of

**Table 1**

Top part: summary of the experimental properties of the 21.47-MeV stretched resonance in  $^{13}\text{C}$  (left), and of its counterparts calculated by the GSM (right) for the  $7/2_7^+$  and the  $9/2_3^+$  states. Bottom part: experimental energies, spin-parity and isospin values of the final states in  $^{12}\text{B}$  and  $^{12}\text{C}$ , and experimental branching ratios of the decay to these states are given in columns 2-4. Equivalent calculated values are provided in columns 5-6. The calculated branchings (for the  $7/2_7^+$  states) are normalized to 100 summing over the same decay paths which were observed in the experiment (i.e., without including the decay to  $2_2^+$  in  $^{12}\text{C}$ , which is unobserved). Calculated spectroscopic factors and partial widths for the proton and neutron decays are provided in the last columns for both states.

$J^\pi = (7/2^+, 9/2^+), T = (1/2, 3/2)$				$J^\pi = 7/2_7^+, T = 1.36$				$J^\pi = 9/2_3^+, T = 1.49$			
$E_{exp} = 21.47$ MeV				$E_{th} = 20.9(5)$ MeV				$E_{th} = 21.8(7)$ MeV			
$\Gamma_{exp} = 270(20)$ keV				$\Gamma_{th} = 400(300)$ keV				$\Gamma_{th} = 150(200)$ keV			
$AZ$	$J^\pi; T$	$E_{exp}$ [MeV]	$BR_{exp}$	$E_{th}$ [MeV]	$BR_{th}$	$S_f$	$\Gamma_p$ [keV]	$S_f$	$\Gamma_p$ [keV]		
$^{12}\text{B}$	$1^-; 1$	2.621		2.810	$0(f_{7/2})$	0	0	0	0		
	$2^-; 1$	1.674	$7(2)^a$	1.979	$3(4)(p_{3/2})$	0.01	$13(6)$	0	0		
					$0(f_{7/2})$	0	0	0	0		
	$2^+; 1$	0.953	$69(6)$	0.867	$60(13)(d_{5/2})$	0.19	$221(48)$	0.22	$60(25)$		
$^{12}\text{C}$	$1^+; 1$	0.0	$<23$	-0.030	$7(5)(d_{5/2})$	0.01	$26(20)$	0	0		
	$2^+; 1$	16.106	$b$	15.7	$2(3)(d_{5/2})$	0.47	$6(10)$	0.67	$80(50)$		
					$1(2)(d_{3/2})$	0.22	$3(6)$	0	0		
	$1^+; 1$	15.110	$24(5)$	14.8	$23(9)(d_{5/2})$	0.08	$86(35)$	0	0		

<sup>a</sup> Undivided branching ratio between  $1^-$  and  $2^-$ .

<sup>b</sup> Not measurable.

the total width  $\Gamma_{th}$ , is of statistical character and arises from uncertainties of the Hamiltonian parameters [36].

The decay pattern inferred from the calculated branchings for the  $7/2_7^+$  resonance is in a very good agreement with the experimental results reported in this paper. The calculated proton emission to the  $2_1^+$ , first-excited state in  $^{12}\text{B}$ , is the strongest channel with branching ratio of  $67(10)$ , which compares well with the  $69(6)$  experimental value. The proton decay to the  $2^-$  state in  $^{12}\text{B}$  is predicted with relative intensity of  $3(4)$ . This result is in agreement with the experimentally-measured relative intensity of  $7(2)$  for the cumulative population of the  $2^-$  and  $1^-$  states in  $^{12}\text{B}$ , not resolved experimentally. A small decay branch of  $7(5)$  to the  $^{12}\text{B}$  ground state is also expected, which is in accordance with the experimental upper limit of 23. We also note that, the  $f$  shells do not play a significant role in the decay path of the M4 resonance.

For the calculated neutron emission from the  $7/2_7^+$  resonance, two branches are found, feeding the  $T = 1$  states. The branching ratio to the  $1^+$  state in  $^{12}\text{C}$  at 15.110 MeV is calculated with a relative intensity of  $23(9)$ , comparable to the experimental value of  $24(5)$ . The GSM also sees a potential decay to the  $2^+$  at 16.106 MeV with relative intensities of  $2(3)$  and  $1(2)$  respectively with the partial waves  $d_{5/2}$  and  $d_{3/2}$ . Experimentally, only the population of the 15.110-MeV state, with relative intensity of  $25(5)$ , was observed, while the decay to the 16.106-MeV state could not be detected, even if existed, due to its very weak  $\gamma$ -branch to the ground state (only 0.27% intensity). Furthermore, the intense alpha-decay branch from the 16.106-MeV level (99.3%) should produce a very broad distribution in the particle spectra, with no peak structure [42], resulting in 1 to 3 counts distributed in the 2-4-MeV energy range, which makes them not recognizable. This is under the assumption of an alpha emission intensity comparable with the proton emission going to  $^{12}\text{B}$ .

In the same manner, partial widths for the  $9/2_3^+$  state were calculated and are given in Table 1. This state has a narrow width of  $150(200)$  keV, but does not decay to the  $1^+$  state at 15.110 MeV in  $^{12}\text{C}$  or to the negative parity states in  $^{12}\text{B}$ . Therefore, the experimental observation of the decay paths leading to the  $1^+$  state in  $^{12}\text{C}$  and to the  $1^-$  or  $2^-$  states in  $^{12}\text{B}$  also excludes the  $9/2_3^+$  assignment to the 21.47-MeV resonance.

We would like to note that also in previous experiments performed with the better energy resolution, like for example in the (e,e') experiment of Ref. [23], only one M4 resonance peak was observed at this range of energy. This observation seemingly contradicts the GSM result which predicts two stretched M4 resonances:

$7/2_7^+$  and  $9/2_3^+$  calculated at 20.9(5) MeV and 21.8(7) MeV excitation energy, respectively. However, within the uncertainties of the Hamiltonian parameters, these two resonances may overlap, which may suggest a possible contribution of the  $9/2_3^+$  M4 resonance in the experimentally observed peak at 21.47 MeV. In such a scenario the calculated branching ratios for the superposed resonances  $7/2_7^+$  and  $9/2_3^+$  would not differ much from that of the  $7/2_7^+$  resonance alone. The only branch allowing to estimate the fraction of the  $9/2_3^+$  state contribution to the peak at 21.47 MeV would be the decay to the  $2_2^+, T = 1$  state at 16.106 MeV in  $^{12}\text{C}$ , as opposed to the case of the  $7/2_7^+$  resonance for which this decay is negligibly small.

However, as it was stated above, the possible decay to the  $2_2^+$  of  $^{12}\text{C}$  is not observable, by  $\gamma$ -ray or alpha detection, both in the present experiment and in future measurements with improved statistics. Given the theoretical analyzes of the 21.47-MeV M4 state in  $^{13}\text{C}$  and current and past experimental observations, the existence of  $7/2^+$  and  $9/2^+$  resonances at similar energy remains a realistic option.

To conclude, the decay of the stretched resonance in  $^{13}\text{C}$ , located at 21.47 MeV with a width of  $270(20)$  keV, was investigated in a (p, p') experiment at 135 MeV. Information on the proton and neutron decay of this state was obtained by measuring particle- $\gamma$  coincidences between inelastically scattered protons populating the stretched state, and  $\gamma$  rays from  $^{12}\text{B}$  and  $^{12}\text{C}$  daughter nuclei. The detected decay, involving  $\gamma$  rays in daughter nuclei, amounts to  $46(10)\%$  of the total decay of the resonance.

The 21.47-MeV stretched resonance in  $^{13}\text{C}$  is an excellent example of an OQS, where individual states couple to states in neighboring nuclei by various decays and captures. Its description requires a full reconstruction of a complicate matrix of couplings between the studied resonance and all states connected by its  $\gamma$  and particle decays. Such a challenge can be taken by the GSM, which allows for a rigorous treatment of bound and unbound nuclear excitations, including coupling to a continuum of non-resonant particles. This approach, here applied for the first time to describe stretched resonances at high excitation energies, provided excellent agreement between the measured and calculated properties of the 21.47-MeV resonance in  $^{13}\text{C}$ , which could originate from two M4 states, closely-lying in energy, with parities  $7/2^+$  and  $9/2^+$ , both with an isospin of  $T = 3/2$ . The detailed description of the decay branching ratios, also obtained for the first time, proves the high quality and precision of the GSM wave-function calculations. Such accuracy is crucial for the correct modeling of the nuclear

structure in the continuum and the understanding of the properties of multi-body states in nuclear OQS and their role in stellar nucleosynthesis.

Further advances in the physics of OQSs require systematic studies of low-lying resonances, including near-threshold states, their complex pattern of decays and captures, and low-energy reactions involving these states. Such investigations will strongly profit from the high-selectivity of state-of-the-art  $\gamma$  tracking arrays, such as AGATA [43–45] and GREINA [46,47] in tracing weak  $\gamma$ -branchings from near-threshold states.

### Declaration of competing interest

The authors declare that they have no known competing financial interests or personal relationships that could have appeared to influence the work reported in this paper.

### Data availability

Data will be made available on request.

### Acknowledgements

We thank N. Michel for fruitful discussions. The project has received funding from the European Union's Horizon 2020 Research and Innovation Programme under Grant Agreements No. 654002 (ENSAR2 project). This work was also supported in part by the Italian Istituto Nazionale di Fisica Nucleare, by the Polish National Science Centre, Poland under research projects No. 2020/39/D/ST2/03443, 2018/31/D/ST2/03009, and No. 2015/17/B/ST2/01534, and by the COPIN and COPIGAL French-Polish scientific exchange programs. M. Sferrazza is supported by the Fonds de la Recherche Scientifique – FNRS under grants numbers J.0174.22 and 4.45.10.08. This work has also benefited from high performance computational resources provided by GANIL.

### References

- [1] E. Caurier, G. Martínez-Pinedo, F. Nowacki, A. Poves, A.P. Zuker, *Rev. Mod. Phys.* **77** (2005) 427.
- [2] L. Coraggio, A. Covello, A. Gargano, N. Itaco, T.T.S. Kuo, *Prog. Part. Nucl. Phys.* **62** (2009) 135.
- [3] T. Otsuka, A. Gade, O. Sorlin, T. Suzuki, Y. Utsuno, *Rev. Mod. Phys.* **92** (2020) 015002.
- [4] C. Forssén, R. Roth, P. Navrátil, *J. Phys. G, Nucl. Part. Phys.* **40** (2013) 055105.
- [5] T. Otsuka, T. Suzuki, J.D. Holt, A. Schwenk, Y. Akaishi, *Phys. Rev. Lett.* **105** (2010) 032501.
- [6] C. Yuan, T. Suzuki, T. Otsuka, F. Xu, N. Tsunoda, *Phys. Rev. C* **85** (2012) 064324.
- [7] M. Ciemala, S. Ziliani, F.C.L. Crespi, S. Leoni, B. Fornal, A. Maj, et al., *Phys. Rev. C* **101** (2020) 021303(R).
- [8] S. Ziliani, M. Ciemala, F.C.L. Crespi, S. Leoni, B. Fornal, T. Suzuki, T. Otsuka, A. Maj, et al., *Phys. Rev. C* **104** (2021) L041301.
- [9] N. Michel, W. Nazarewicz, M. Płoszajczak, K. Bennaceur, *Phys. Rev. Lett.* **89** (2002) 042502.
- [10] N. Michel, W. Nazarewicz, M. Płoszajczak, J. Okołowicz, *Phys. Rev. C* **67** (2003) 054311.
- [11] N. Michel, W. Nazarewicz, M. Płoszajczak, *Phys. Rev. C* **70** (2004) 064313.
- [12] R. Id Betan, R.J. Liotta, N. Sandulescu, T. Vertse, *Phys. Rev. Lett.* **89** (2002) 042501.
- [13] R. Id Betan, R.J. Liotta, N. Sandulescu, T. Vertse, *Phys. Rev. C* **67** (2003) 014322.
- [14] N. Michel, W. Nazarewicz, M. Płoszajczak, T. Vertse, *J. Phys. G, Nucl. Part. Phys.* **36** (2009) 013101.
- [15] N. Michel, M. Płoszajczak, *Gamow Shell Model – The Unified Theory of Nuclear Structure and Reactions*, vol. 983, Springer, 2021, <https://www.springer.com/gp/book/9783030693558>.
- [16] C.E. Hyde-Wright, et al., *Phys. Rev. C* **35** (1987) 880.
- [17] S. Yen, R. Sobie, H. Zarek, B.O. Pich, T.E. Drake, C. Williamson, S. Kowalski, C. Sargent, *Phys. Lett. B* **93** (1980) 250.
- [18] S. Raman, L.W. Fagg, R.S. Hicks, Giant magnetic resonances, in: J. Speth (Ed.), *Electric and Magnetic Giant Resonances in Nuclei*, World Scientific Publishing Company, 1991.
- [19] A.N. Golzov, N.G. Goncharova, H.R. Kissener, *Nucl. Phys. A* **462** (1987) 376.
- [20] J. Dehnhard, S.J. Tripp, M.A. Franey, G.S. Kyle, C.L. Morris, R.L. Boudrie, J. Piffaretti, H.A. Thiessen, *Phys. Rev. Lett.* **43** (1979) 1091.
- [21] J. Seestrom-Morris, D. Dehnhard, M.A. Franey, G.S. Kyle, C.L. Morris, R.L. Boudrie, J. Piffaretti, H.A. Thiessen, *Phys. Rev. C* **26** (1982) 594.
- [22] S.F. Collins, G.G. Shute, B.M. Spicer, V.C. Officer, D.W. Devins, D.L. Friesel, W.P. Jones, *Nucl. Phys. A* **481** (1988) 494.
- [23] R.S. Hicks, R.A. Lindgren, M.A. Plum, G.A. Peterson, H. Crannell, D.I. Sober, H.A. Thiessen, D.J. Millener, *Phys. Rev. C* **34** (1986) 1161.
- [24] E. Korkmaz, et al.,  $^{12}\text{C}(p, \pi^+n)$  Coincidence Measurement, Indiana University Cyclotron Facility Scientific and Technical report, 1986, p. 67; E. Korkmaz, et al.,  $^{12}\text{C}(p, \pi^+n)$  Coincidence Measurement, Indiana University Cyclotron Facility Scientific and Technical report, 1987, p. 65.
- [25] J. Łukasik, et al., *Nucl. Instrum. Methods Phys. Res., Sect. A* **709** (2013) 120.
- [26] A. Giaz, L. Pellegrini, S. Riboldi, F. Camera, et al., *Nucl. Instrum. Methods Phys. Res., Sect. A* **729** (2013) 910.
- [27] A. Maj, F. Azaiez, D. Jenkins, C. Schmitt, O. Stezowski, J.P. Wieleccko, *Acta Phys. Pol. B* **40** (2009) 565, and <http://paris.ifj.edu.pl>.
- [28] N. Cieplicka-Oryńczak, D. Mengoni, M. Ciemala, S. Leoni, B. Fornal, et al., *Eur. Phys. J. A* **54** (2018) 209.
- [29] J. Okołowicz, M. Płoszajczak, I. Rotter, *Phys. Rep.* **374** (2003) 271.
- [30] G. Papadimitriou, A.T. Kruppa, N. Michel, W. Nazarewicz, M. Płoszajczak, J. Rotureau, *Phys. Rev. C* **84** (2011) 051304(R).
- [31] N. Michel, W. Nazarewicz, M. Płoszajczak, J. Rotureau, *Phys. Rev. C* **74** (2006) 054305.
- [32] G. Papadimitriou, J. Rotureau, N. Michel, M. Płoszajczak, B.R. Barrett, *Phys. Rev. C* **88** (2013) 044318.
- [33] K. Fossez, J. Rotureau, N. Michel, M. Płoszajczak, *Phys. Rev. Lett.* **119** (2017) 032501.
- [34] H. Furutani, H. Horiuchi, R. Tamagaki, *Prog. Theor. Phys.* **62** (1979) 981.
- [35] H. Furutani, H. Kanada, T. Kaneko, S. Nagata, H. Nishioka, S. Okabe, S. Saito, T. Sakuda, M. Seya, *Theor. Phys. Suppl.* **68** (1980) 193.
- [36] Y. Jaganathen, R.M. Id Betan, N. Michel, W. Nazarewicz, M. Płoszajczak, J. Rotureau, *Phys. Rev. C* **96** (2017) 054316.
- [37] N. Michel, W. Nazarewicz, M. Płoszajczak, *Nucl. Phys. A* **794** (2007) 29.
- [38] R.J. Furnstahl, H.W. Hammer, *Phys. Lett. B* **531** (2002) 203.
- [39] T. Duguet, H. Hergert, J.D. Holt, V. Somà, *Phys. Rev. C* **92** (2015) 034313.
- [40] M. Gómez-Ramos, A. Obertelli, Y.L. Sun, *Eur. Phys. J. A* **57** (4) (2021) 148, <https://doi.org/10.1140/epja/s10050-021-00446-3>.
- [41] J. Okołowicz, N. Michel, W. Nazarewicz, M. Płoszajczak, *Phys. Rev. C* **85** (2012) 064320.
- [42] K.L. Laursen, H.O.U. Fynbo, O.S. Kirsebom, K.S. Madsbøll, K. Riisager, *Eur. Phys. J. A* **52** (2016) 271.
- [43] S. Akkoyun, et al., *Nucl. Instrum. Methods Phys. Res., Sect. A* **668** (2012) 26.
- [44] E. Clément, C. Michelagnoli, G. de France, H.J. Li, A. Lemasson, et al., *Nucl. Instrum. Methods Phys. Res., Sect. A* **855** (2017) 1.
- [45] W. Korten, et al., *Eur. Phys. J. A* **56** (2020) 137.
- [46] S. Paschalis, I.Y. Lee, A.O. Macchiavelli, *Nucl. Instrum. Methods Phys. Res., Sect. A* **709** (2013) 44.
- [47] P. Fallon, A. Gade, I.-Y. Lee, *Annu. Rev. Nucl. Part. Sci.* **66** (2016) 321.